Journal of Thermal Analysis and Calorimetry, Vol. 77 (2004) 341–351

DSC STUDIES ON LONG-TERM PROPERTIES OF NITROCELLULOSE AND *SYM*-DIPHENYLUREA SYSTEM

A. Książczak and M. Ostrowski*

Department of Chemistry, Warsaw University of Technology, Noakowskiego 3, 00-664 Warsaw, Poland

Abstract

Long-term investigations of the phase structure and pore structure of nitrocellulose and *sym*-diethyldiphenylurea (C1) mixtures were conducted for samples with C1 mass fractions w_{C1}=0.5, 0.6 and 0.8. The distribution of pore sizes and the composition of the nitrocellulose matrix were determined based on the melting enthalpy of C1. The three kinds of pores was observed with the characteristic size of about 7, 14 and 28 nm. Long-term storage of mixtures caused an increase in size of the smallest pores and a decrease of C1 concentration in the nitrocellulose matrix. The mechanism of changes in pore sizes is presented in term of multi-sheet model of NC fiber.

Keywords: diethyldiphenylurea, DSC, melting enthalpy, nitrocellulose, pore structure, thermoporosimetry

Introduction

Nitrocellulose (NC, cellulose nitrate) is one of the longest applied polymers in many technologies [1]. It was the main raw material for the oldest plastic – celluloid. It is still utilised in varnish manufacture, explosives, selective membranes and filters used in microbiology as well as in the production of ion track detectors. The glass transition of NC is close to its decomposition temperature. That is why this polymer has to be processed with an addition of low molecular compounds acting as plasticizers, solvents and stabilisers. NC is obtained in the process of nitrating cellulose. The main elements of NC fibre structure are similar to those of cellulose fibre structure [2]. The pore structure of NC enables the low molecular compound to penetrate into the existing fibre structures. Knowing how these structures are built is very important from a practical point of view.

We investigated the binary mixtures of NC + *sym*-diethyldiphenylurea (C1) [3, 4], and NC + 2,6-dinitrotoluene [5] using DSC calorimetry in our previous works. The dependence of mixing enthalpy upon concentration [3] in the NC + C1 system was determined and was later utilized to establish the concentrational dependence of the glass transition temperature and the phase diagram [4] of the NC + C1 system. In the NC +

* Author for correspondence: andrzks@ch.pw.edu.pl

1388–6150/2004/ $ 20.00

Akadémiai Kiadó, Budapest
Kluwer Academic Publishers, Dordrecht

2,6-dinitrotoluene system the concentrational dependence of mixing enthalpy was determined and the changes of pore structure in the mixtures were described [5]. The pore structure of NC in water was investigated using thermoporometric method [6]. The aim of this work is to determine the influence of time on the composition of the nitrocellulose matrix and the pore structure of NC + C1 mixtures.

Experimental

The nitrocellulose utilised in this investigation was produced from sulfite pulp in Pionki Polymer Plant. According to the producer's specifications it contained 13.51% of nitrogen. The material obtained from manufacturer was dried to constant mass under the vacuum. The properties of the NC were investigated with the BJH adsorption-desorption method. The mean surface of fibres was 9.0 $m^2\ g^{-1}$, mean pore volume was 0.023 $cm^3\ g^{-1}$ and mean pore diameter was 10.2 nm. The above measurements were carried out on MICROMETRICS apparatus ASAP 2405.

S-diethyldiphenylurea (C1) was crystallised many times from ethanol. Its purity was determined by the cryometric method and was equal 99.9% mole. C1 was ground in an agate mortar and mixed with appropriate mass amounts of nitrocellulose. Several grams of mixtures with mass fractions of C1 w_{C1} = 0.5001, 0.5975, 0.7995 were obtained. Samples with masses of about 20–40 mg were taken from these mixtures and pressed under a pressure of about 0.5 GPa into tablets with the dimensions and shape of aluminium calorimetric pans. The samples were sealed hermetically in pans under reduced pressure to about 1.3 kPa.

Measurements were carried out on Perkin Elmer Pyris DSC 1 calorimeter in the temperature range of 298–380 K (the heating rate was equal 2 K min^{-1}). The aparatus was power compensate type. In order to initiate the C1 crystallisation process the samples were cooled by putting them to the surface of ice after each measurement. They were stored in room temperature and reused for successive measurements after specified periods of time (from a few days to about one year).

The thermoporosimetric coefficients were determined based on DSC measurements registered for mixtures of equal masses of C1 and ceramic porous material with specified pore sizes. The measurement conditions (temperature range, heating rate) were identical as in measurements performed for the investigated NC + C1 mixtures.

Method background

The self-acting mixing of mixture components proceeded during the first measurement carried out on the sample. The mixing enthalpy and the intermolecular interaction parameters were estimated from these measurements. Results of such an investigation performed on NC with a 13.2% nitrogen content and C1 were presented in our previous works [3, 4]. The phase and pore structure of samples were determined based on subsequent measurements registered for each sample. The mass fraction of C1, w_{C1}^{cryst}, which crystallised from the polymeric matrix during storage, was defined based on the thermal effect of C1 melting $Q(t)$ for defined storage period t:

$$w_{C1}^{cryst} = Q(t) / \Delta H° \quad (1)$$

where $\Delta H°$ is the melting enthalpy of pure C1 in unrestricted space. This composition is different from the summary mass fraction of C1 in sample w_{C1}, because part of the low-molecular compound is bounded in the NC matrix. The thermodynamically stable state of system at final temperature of calorimetric measurement T_f according phase diagram [4] is one phase solution for most of concentrations. However NC structure is retained in relatively high temperature. Probably the sample is in this temperature to short to loose orginal NC structure completely during the measurement. Better description of the system at T_f, especialy for medium C1 concentrations, is heavily swelled NC fibre. The system in the storage temperature should consist of two phases of pure components. Nevertheless complete crystallisation of C1 is not observed – part of C1 molecules is still bounded in swelled NC. Even if the phase decomposition occurs completely, some of C1 will not crystallize because it will be ordered at the NC surface. The C1 mass fraction bound in the polymeric matrix can be calculated from the following equation:

$$w_{C1}^{bound} = w_{C1} - w_{C1}^{cryst} \quad (2)$$

The amount of non-crystallising C1 molecules equivalent to a NC unit in the nitrocellulose matrix can be computed on the basis of this mass fraction:

$$n = w_{C1}^{bound} / (M_{NC} / M_{C1})(1 - w_{C1}) \quad (3)$$

Substituting Eqs (1) and (2) to (3) we obtain:

$$n = (w_{C1} - Q(t) / \Delta H°) / (M_{NC} / M_{C1})(1 - w_{C1}) \quad (4)$$

where n is the amount of C1 molecules equivalent to a NC unit in the nitrocellulose matrix, and M_{NC} and M_{C1} are the molar mass of the NC unit and C1 appropriately. This parameter will be used to characterise the nitrocellulose matrix after a specific period of sample storage.

DSC measurements serve to define not only the phase composition of the sample but also its morphological structure. The same measurements, whose analysis produces a description of the sample's phase composition, serve to determine the dimensions of the confined spaces that are created in the sample and filled by crystalline C1. This can be observed by applying thermoporosimetry [7].

The displacement of C1 molecules from the NC matrix during storage changes the phase composition and pore structure. According to the phase diagram presented in work [4], storing the sample at room temperature (which is below the eutectic point) yields C1 crystallisation. Pores are filled by crystalline C1. The melting temperature of C1 in pores (confined spaces) is lower than the melting point of C1 in unconfined space (bulk melting). This phenomenon serves as the basis of the thermoporosimetric method of determining pore dimensions. The dependence of pore dimension R on the decrease of melting temperature ΔT [7] is described by the following equation:

$$R = A / \Delta T + B \quad (4)$$

where A and B are the thermoporosimetric constants for the system. The parameters of Eq. (4) can be determined for a chosen liquid that fills pores based on DSC measurements of the melting process in porous material with specified pore dimensions. The constant B describes the thickness of the layer of molecules of the liquid close to the pore wall surface that is not subjected to phase transition. It is generally accepted that the thickness of this layer is from one to three molecules. The value of this constant is much lower than $A/\Delta T$ term for the investigated samples. Omitting this value when determining pore dimensions is not a big error. The value of constant A determined based on calibrating measurements of the C1 – ceramic material mixture was equal 217.7 K nm.

The DSC curves of the melting process serve to determine pore size distribution in the sample using the following equation:

$$\mathrm{d}V/\mathrm{d}R = (ky / W_\mathrm{a}) / (A/\Delta T^2) \tag{5}$$

where y is the calorimetric signal, k – calibrating constant of the apparatus, A – thermoporosimetric constant from Eq. (4), $\Delta T = T^\mathrm{o}_\mathrm{m} - T$ – difference between the melting point of bulk C1 and C1 in confined space. The calorimetric signal in power compensation type calorimeter is the thermal effect, which have to be supplied or received to the sample in the unit of time to balance the thermal effect evolved in the sample. The software provided with our apparatus gives experimental data expressed in mW, taking into account the calibration and we used value of calibrating constant $k = 1$. The values of y substituted in Eq. (5) should be expressed in J K^{-1}. We divided experimental values of DSC signal by heating rate to obtain proper units. The apparent heat of melting W_a was calculated using experimental temperature dependence of heat capacity of C1 and heat of fusion of C1:

$$W_\mathrm{a}(T) = -6.505\cdot10^{-7}\left(T^{\mathrm{o}\,3}_\mathrm{m} - T^3\right) + 2.522\cdot10^{-3}\left(T^{\mathrm{o}\,2}_\mathrm{m} - T^2\right) - 1.853\left(T^\mathrm{o}_\mathrm{m} - T\right) + 110 \tag{6}$$

where T^o_m is the normal temperature of C1 melting in unrestricted space. The dependence was multiplied by C1 density d = 1.14 g cm^{-3} [9] to have proper units in Eq. (5). The thermoporosimetric method can be utilised to determine pore sizes from 2 to 150 nm.

The pore volume in the sample can be estimated through numerical integration of the pore size distribution curve (Eq. 5) in the range 5–150 nm:

$$V = \int_5^{150}\left(\mathrm{d}V/\mathrm{d}R\right)\mathrm{d}R \tag{7}$$

Results

The typical DSC curves for the sample with C1 mass fraction $w_{\mathrm{C1}} = 0.5001$ for different storage times are presented at Fig. 1. There was no melting effect observed for short storage periods. The thermal effect of melting registered after 6 days of storage was very small, and the proper analysis of it was impossible (curve 1). The sharp peak connected with the melting process of bulk C1 appears in the case of longer storage periods. The two broad peaks are an effect of melting processes in confined

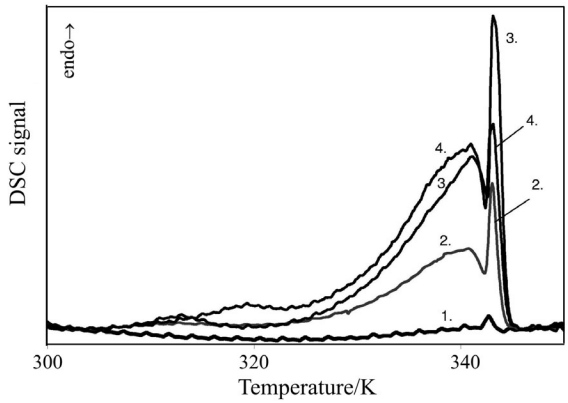

Fig. 1 DSC C1 melting curves of sample $x_{wC1} = 0.5001$ after the following storage periods: 6 days (curve 1), 42 days (curve 2), 75 days (curve 3), 309 days (curve 4)

spaces with different sizes. The temperature of the low-temperature peak maximum increases with storage. The temperatures of the high- and medium-temperature peak maximums are roughly constant. The total melting enthalpy increases when the storage period is extended. This is due to C1 migration from the polymeric matrix to unconfined and confined spaces.

The DSC curves registered for the mixture with the mass fraction of C1 $w_{C1} = 0.5975$ for different storage periods are presented together in Fig. 2. There were no thermal effects for very short periods of storing (curves not presented). The DSC curves for very long storage periods contain 3–4 melting peaks. The low-temperature maximum, as in the case of the previously discussed mixture, shifts to higher temperatures, and its thermal effect increases when the storage period is extended. The temperature of the middle peak maximum for a storage time of 27 days was equal 335K. This peak shifted toward lower temperatures (about 333 K) in the case of longer storage periods in subsequent measurements. The fourth sharp peak, connected with the bulk C1 melting process, appears at a temperature of 345 K for a storage time of about one year.

The DSC curves for the mixture with $w_{C1} = 0.7995$ are presented in Fig. 3. The curves possess three endothermic peaks, as in the case of the previously discussed mixtures. The shift of the low-temperature peak resembles the changes in the low-temperature peak observed in the previously discussed mixtures. The middle peak is considerably lower than in mixtures with a lower C1 content but it remains practically identical in all measurements. The behaviour of the high-temperature peak is different. Its height depends on the total time from preparing the sample to the discussed measurement, independent of storage time between two consecutive measurements. This peak is the highest in the third measurement, for a long storage period (242 days). It practically does not change in subsequent measurements, despite significant differences in storage time. A small fourth peak on the high-temperature

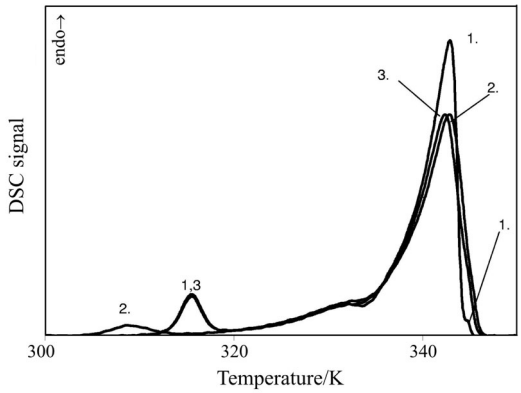

Fig. 2 DSC C1 melting curves of sample $x_{wC1} = 0.5975$ after the following storage periods: 27 days (curve 1), 294 days (curve 2), 426 days (curve 3)

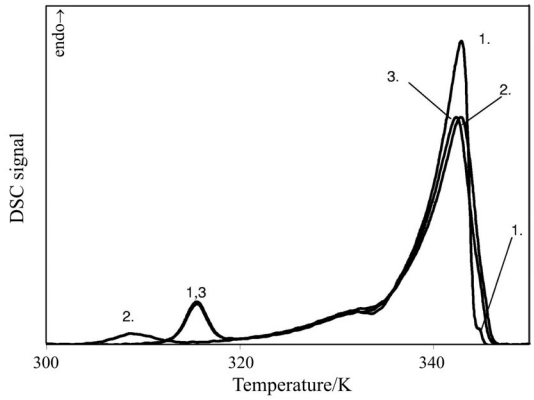

Fig. 3 DSC C1 melting curves of sample $x_{wC1} = 0.7995$ after the following storage periods: 242 days (curve 1, 3rd scan), 7 days (curve 2, 4th scan), 292 days (curve 3, 5th scan)

shoulder of this peak appears in the third measurement. It can be interpreted as the melting peak of bulk C1.

The parameter n is higher when the mass fraction of C1 is larger. The dependence of parameter (n) upon storage time for the sample with the mass fraction $w_{C1} = 0.5001$ is presented in Fig. 4 (empty circles). Increasing the sample's storage period decreases the n amount of C1 molecules per NC unit. The parameter n achieves a certain constant value of about 0.80 for storage periods of more than 100 days. The values of parameter n calculated for the mixture with the mass fraction of C1 $w_{C1} = 0.5975$ for different storage periods are much bigger than for the mixture with $w_{C1} = 0.5001$. These values decrease with an increase of storage time, which is presented in Fig. 4 (filled square points). The parameter n calculated for the mixture with the mass fraction $w_{C1} = 0.7995$ is the biggest and it decreases slowly with stor-

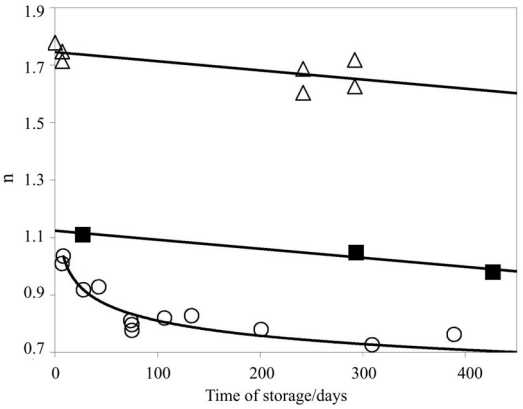

Fig. 4 Dependence of parameter *n* upon storage time for samples x_{wC1} = 0.5001 (circles), 0.5975 (squares), 0.7995 (triangles)

age. These results are presented in Fig. 4 with triangle points. Analysis of changes in the value of *n* according to storage time in the initial period shows that these changes are most significant in the case of lower C1 mass fractions. These results testify that the rate of C1 migration is larger for smaller w_{C1}.

The pore size distribution curve for the sample with the mass fraction w_{C1} = 0.5001 and the storage time equal 43 days, which was calculated based on the DSC curve (curve 1, Fig. 1), is presented in Fig. 5. The characteristic size of the smallest pores increases with an increase in storage time. These changes are presented in Fig. 2 (circles). This maximum on the distribution curve is very sharp and is the highest on the curve. The second maximum corresponds to the characteristic size of pores 20.6 ± 1.0 nm.

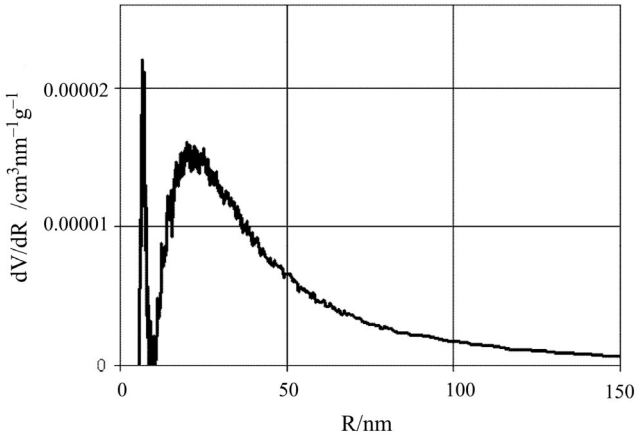

Fig. 5 Distribution of pore dimensions for sample x_{wC1} = 0.5001 after a storage period of 43 days

The distributions of pore sizes for the mixture with $w_{C1} = 0.5975$ possess two distinct peaks presented in Fig. 6 for two measurements. The smallest pores increase their characteristic size from 6.7 to 8.1 nm with an increase in storage time. The dependence of the size of these pores upon storage time is presented in Fig. 7 (filled squares). It is worth emphasizing that their participation increases with an increase of the storage time. The characteristic values of the medium and the biggest pores for this mass fraction are with good approximation independent of the storage time. The sizes are presented in Table 1. The characteristic sizes corresponding to the first maximum on the curve of pore size distribution (the smallest pores) for the mixture with the mass fraction $w_{C1} = 0.7995$ increase with storage from 5.9 to 8.1 nm. The characteristic sizes of medium and big pores practically do not change during storage (Table 1).

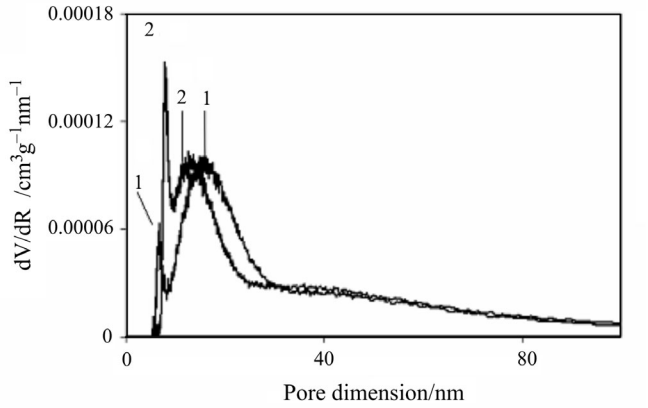

Fig. 6 Distribution of pore dimensions for sample $x_{wC1} = 0.5975$ after storage periods of 27 days (curve 1) and 294 days (curve 2)

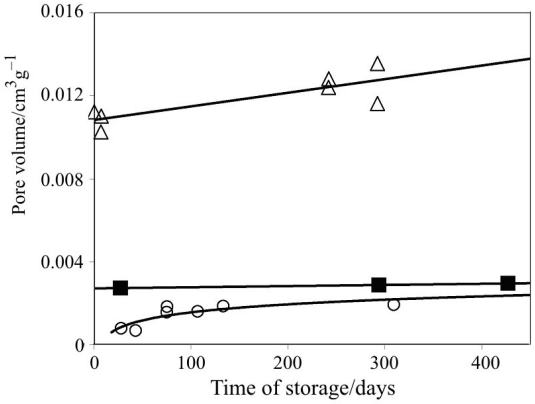

Fig. 7 Dependence of pore volume upon storage time in samples $x_{wC1} = 0.5001$ (circles), 0.5975 (squares), 0.7995 (triangles)

Table 1 Mean pore sizes for different mass fractions

x_{wC1}	Mean pore size of medium pores/nm	Mean pore size of large pores/nm
0.5001	–	20.6
0.5975	13.8	36.1
0.7995	14.7	28.3

The volumes of pores increase when the mass fraction of C1 is increased. The pore volume in the sample with $w_{C1} = 0.5001$ increases when the storage time is extended to 100 days, and then stops at the level of $(2.2 \pm 0.2)\cdot10^{-3}$ cm^3 g^{-1} (Fig. 8, unfilled circles). The pore volume of other discussed mixtures with bigger C1 content changes slightly with storage (Fig. 8).

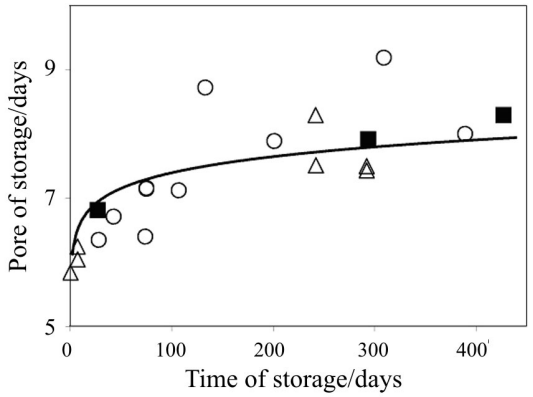

Fig. 8 Dependence of the characteristic size of the smallest pores upon storage time of samples $x_{wC1} = 0.5001$ (circles), 0.5975 (filled squares), 0.7995 (triangles)

Discussion

The origin of pores in the samples can be connected with the original structure of nitrocellulose fibers. Pores in cellulose pulps are created in spaces, from which the non-cellulosic components (hemicelluloses, lignins) were eliminated [8]. Pore walls are built from microfibrils – morphologies created with parallelly packed cellulosic chains. Microfibrils can join with each other forming planes (sheets). There are empty spaces (pores) between such planes. C1 melts during the first measurement, and the low-molecular compound penetrates different structures of the fibre when the temperature of the sample linearly increases to the final temperature of the measurement (380 K). The eutectic temperature estimated based on the Flory–Huggins parameter is equal T_e=313.8 K [4] and is higher than the temperature at which the samples are stored. This means that when samples are stored C1 should migrate from the NC matrix to the confined areas in the pores.

The addition of the low-molecular compound, i.e. C1, causes an initial swelling of the fibres. This in turn decreases the smallest pore size. Long-term storage of the samples can bring about changes in pore characteristics of the samples. The smallest pores grow wider and increase their size to the pore sizes present in pure NC (~10 nm) (Fig. 8). The question arises, how are medium and big size pores formed. Analysis of their characteristic sizes shows that their values are multiples of the values of characteristic sizes of smaller pores. The multiplication of characteristic pore sizes of medium and small pores can be interpreted as a result of the joining of planes. This can yield dual sizes of pores. The joining of the planes can lead to the migration of C1 outside of the fibre and its crystallisation in unconfined spaces. Melting of the layer of crystalline C1 between the bottom of the calorimetric span and the surface of the investigated sample probably causes the sharp high temperature peaks.

The volumes of pores obtained for samples with different C1 contents for a storage time of about 300 days are presented in Table 2. The results presented in Table 2 show that an increase of C1 mass fraction causes a subsequent increase of pore volume. The volumes are distinctly lower than the NC volume determined by the BJH adsorption-desorption method (0.02 $cm^3\ g^{-1}$). The comparison of these results shows that in the case of the investigated mixtures pores existing in pure NC used in the measurements were only partially filled.

Table 2 Pore volumes for different mass fractions with a storage time of approx. 300 days

x_{wC1}	Pore volume / $cm^3\ g^{-1}$
0.5001	0.0019
0.5975	0.0028
0.7995	0.0135

Conclusions

DSC investigations carried out in this study show that changes observed during long periods of storing NC + C1 mixtures at room temperature are connected with the migration of C1 from the NC matrix to the confined areas (pores). The smallest pores are about 7.5 nm and increase when the storage time is extended. Medium pores are about 14 nm and big pores are about 28 nm. It can be accepted that the size of medium and big pores are multiples of the size of small pores. These results suggest that bigger pores are created as a result of the joining of planes creating smaller pores. The joining of the planes – walls of medium pores doubles their size and leads to the creation of big pores. It should be assumed that the joining of planes that constitute the walls of big pores should in turn produce pores twice the size of those before the interaction. These pores cannot be observed by the thermoporosimetric method, because the C1 melting point depression is too low to be observed. Subsequent joining of planes can lead to a situation in which, after an appropriately long enough storage time, the C1 melting process should proceed in the unconfined space. The compari-

son of pore volumes in the investigated samples and in the pure NC used in preparing the samples indicates that pores in NC mixtures are only partially filled.

References

1 F. D. Miles, Cellulose Nitrate, Oliver and Boyd, London-Edinburgh 1955, pp. 42, 124, 206, 233.
2 T. Urbański, Chemistry and Technology of Explosives, Vol. 2, 1st edition, Pergamon Press, Oxford-New York-Toronto-Sidney-Paris-Frankfurt, 1984, pp. 234–242.
3 A. Książczak and T. Książczak, J. Therm. Anal. Cal., 54 (1998) 323.
4 A. Książczak, T. Książczak and M. Ostrowski, J. Therm. Anal. Cal., 74 (2003) 575.
5 A. Książczak and T. Wolszakiewicz, J. Therm. Anal. Cal., 67 (2002) 751.
6 A. Książczak, A. Radomski and T. Zielenkiewicz, J. Therm. Anal. Cal., 74 (2003) 559.
7 B. Brun, A. Lallemand, J.-F. Quinson and V. Eyraud, Thermochim. Acta, 21 (1977) 59.
8 J. E. Stone and A. M. Scallan, Pulp Paper Magazine Canada, 66 (1965) T407.
9 T. H. Huang, S. T. Thynell and K. K. Kuo, J. Propul. Power, 11 (1995) 781.